Effects of Dissipative Energy Loss in Dampened Simple Harmonic Oscillation

Arnav Sharma
Ozan Bicakci

12 November 2025

Abstract

The motion of a vertically oscillating mass-spring system depends on several variables, such as the spring constant k, damping coefficient b, angular frequency ω, and damping ratio α. Both undamped and damped oscillations were analyzed for various configurations to test the equations of simple harmonic motion and with the assumption that Stokes' drag is a good approximation of the drag force we observe (or that $f = -bv$). The primary objectives were to verify whether $x(t) = Ae^{-\alpha t}\cos(\omega t + \phi)$ models our observations well, whether $\omega = \sqrt{\omega_0^2 - \alpha^2}$ models frequency shifts well, and determine how mass and damping influence oscillation parameters. With week 1 having only single-fit data and week 2 multiple, reassessment using Week 2 standard deviations applied to Week 1 fit values allowed further agreement across measurements. Histograms of α and ω displayed approximately Gaussian distributions with slight skewness or flattening, consistent with the limited number of trials (20) and the Central Limit Theorem [3]. Overall, the results confirm that while the damped harmonic oscillator model accurately describes the system, systematic effects such as mass-dependent spring deviations and plate orientation dominate the observed discrepancies.

1 Introduction

The motion of a mass attached to a vertical spring can be described using Newton's second law under the assumption that there exists a restoring spring force, no gravitational force in consideration (because we start oscillation from equilibrium), and a case-by-case basis of an additional damping force from air resistance.

For an ideal, undamped system, the only force on the mass is the restoring spring force as modeled by Hooke's Law, $F = -kx$, with k as the spring constant and x as the displacement from equilibrium. Applying Newton's second law, $F = ma$, gives:

$$m\frac{d^2x}{dt^2} = -kx$$

$$\frac{d^2x}{dt^2} + \frac{k}{m}x = 0$$

$$x(t) = A\cos(\omega_0 t + \phi)$$

where $\omega_0 = \sqrt{\frac{k}{m}}$ is the natural angular frequency, A is the amplitude, and ϕ is the phase constant due to specific initial conditions.
We can then derive the period as:

$$W = \frac{2\pi}{\omega_0} = 2\pi\sqrt{\frac{m}{k}}$$

Now, when damping is introduced, a resistive force proportional to the velocity acts on the mass:

$$F_d = -b\frac{dx}{dt}$$

where b is the damping constant. The net force on the mass then becomes:

$$m\frac{d^2x}{dt^2} = -kx - b\frac{dx}{dt}$$

$$\frac{d^2x}{dt^2} + \frac{b}{m}\frac{dx}{dt} + \frac{k}{m}x = 0$$

And with $\alpha = \frac{b}{2m}$ and $\omega_0^2 = \frac{k}{m}$, we can write:

$$\frac{d^2x}{dt^2} + 2\alpha\frac{dx}{dt} + \omega_0^2 x = 0$$

After finding the characteristic equation of this differential equation, depending on the discriminant, we have 3 cases:

- **Underdamped:** $\alpha < \omega_0$: an exponentially decaying amplitude.
- **Critically damped:** $\alpha = \omega_0$: quickly returning to equilibrium with no oscillation.
- **Overdamped:** $\alpha > \omega_0$: slow return to equilibrium with no oscillation.

In the underdamped case, which we will use later on, the solution is:

$$x(t) = Ae^{-\alpha t}\cos(\omega t + \phi)$$

where

$$\omega = \sqrt{\omega_0^2 - \alpha^2}$$

Our apparatus consists of a vertical spring with 2 masses (100g and 250g) and 2 plates (a small plate and another large) and with our procedure testing 5 of the many possible combinations of configurations we could have given these. In our procedure, we attach our mass and let it settle itself into equilibrium position. Then with a slight displacement, we record the oscillation motion using a motion sensor and repeat 20 times with this specific configuration.

We then repeat this procedure for all 5 configurations, and record all measurements for further analysis. After using nonlinear least-squares fitting to extract the parameters of our underdamped equation, we can further calculate and do analysis on other relevant values affecting our motion.

2 Measurements and Analysis

After measuring 100 total trials, we analyze the associated datasets using the python scipy library to get the following data:

Table 1: Measured decay constants α for each configuration.

Configuration	m (g)	α (s^{-1})	Std. Dev.
100 g, no plate	102.4	0.006064	0.000380
100 g, small plate	110.9	0.042645	0.000907
250 g, no plate	253.4	0.005029	0.000394
250 g, small plate	256.9	0.020530	0.000475
250 g, large plate	268.2	0.037032	0.000681

Table 2: Measured natural angular frequencies ω_0 for each configuration.

Configuration	m (g)	ω_0 (rad/s)	Std. Dev.
100 g, no plate	102.4	7.156623	0.000371
100 g, small plate	110.9	6.823436	0.000869
250 g, no plate	253.4	4.660163	0.000711
250 g, small plate	256.9	4.571114	0.000329
250 g, large plate	268.2	4.493950	0.000769

Given the relationships, b = (2m)α, where b is the drag force constant, we can find the calculated value for each of the 5 configurations and their uncertainties using the following error propagation:

$$\sigma_b^2 = \left(\frac{\partial b}{\partial m}\right)^2 \sigma_m^2 + \left(\frac{\partial b}{\partial \alpha}\right)^2 \sigma_\alpha^2,$$

where σ_m and σ_α are the uncertainties in the measured mass and in α, respectively.
For $b = 2m\alpha$ the partial derivatives are

$$\frac{\partial b}{\partial m} = 2\alpha, \qquad \frac{\partial b}{\partial \alpha} = 2m.$$

Substituting these into the propagation formula gives

$$\sigma_b^2 = (2\alpha)^2 \sigma_m^2 + (2m)^2 \sigma_\alpha^2 = 4\alpha^2\sigma_m^2 + 4m^2\sigma_\alpha^2.$$

However, in our analysis we assume the mass measurement uncertainty is negligible compared to the uncertainty of the drag constant σ_α, yielding us with:

$$\sigma_b = 2m\,\sigma_\alpha \ ,$$

Given these, we can now calculate all the values of the drag constant as below:

Table 3: Drag coefficient b for each configuration with propagated uncertainties.

Configuration	m (g)	b (kg/s)	σ_b (kg/s)
100 g, no plate	102.4	0.00124	0.00008
100 g, small plate	110.9	0.00946	0.00020
250 g, no plate	253.4	0.00255	0.00020
250 g, small plate	256.9	0.01055	0.00024
250 g, large plate	268.2	0.01986	0.00037

Using the same process for $k = m\,\omega_0^2$ and given that $\omega_0 = \sqrt{\omega^2 + \alpha^2}$, the uncertainty in ω_0 can be calculated using standard error propagation:

$$\sigma_{\omega_0}^2 = \left(\frac{\partial \omega_0}{\partial \omega}\right)^2 \sigma_\omega^2 + \left(\frac{\partial \omega_0}{\partial \alpha}\right)^2 \sigma_\alpha^2,$$

where the partial derivatives (using chain rule) are

$$\frac{\partial \omega_0}{\partial \omega} = \frac{\omega}{\sqrt{\omega^2 + \alpha^2}} = \frac{\omega}{\omega_0}, \qquad \frac{\partial \omega_0}{\partial \alpha} = \frac{\alpha}{\sqrt{\omega^2 + \alpha^2}} = \frac{\alpha}{\omega_0}.$$

Substituting gives

$$\sigma_{\omega_0} = \sqrt{\left(\frac{\omega}{\omega_0}\sigma_\omega\right)^2 + \left(\frac{\alpha}{\omega_0}\sigma_\alpha\right)^2}.$$

Now given $k = m\,\omega_0^2$, to calculate its uncertainty, we propagated as follows:

$$\sigma_k^2 = \left(\frac{\partial k}{\partial m}\right)^2 \sigma_m^2 + \left(\frac{\partial k}{\partial \omega_0}\right)^2 \sigma_{\omega_0}^2,$$

with

$$\frac{\partial k}{\partial m} = \omega_0^2, \qquad \frac{\partial k}{\partial \omega_0} = 2m\,\omega_0.$$

Since the uncertainty in the mass is negligible compared to the uncertainty in ω_0, we finally obtain

$$\sigma_k = 2m\,\omega_0\,\sigma_{\omega_0} = 2m\,\omega_0 \sqrt{\left(\frac{\omega}{\omega_0}\sigma_\omega\right)^2 + \left(\frac{\alpha}{\omega_0}\sigma_\alpha\right)^2}$$

Using these results, we get the table of values:

Table 4: Calculated spring constants k for each configuration with propagated uncertainties.

Configuration	m (g)	k (N/m)	σ_k (N/m)
100 g, no plate	102.4	5.24465	0.00054
100 g, small plate	110.9	5.16342	0.00131
250 g, no plate	253.4	5.50312	0.00168
250 g, small plate	256.9	5.36795	0.00077
250 g, large plate	268.2	5.41646	0.00185

Now given Table 4, we can determine whether the spring constant k varied significantly across the different configurations by doing pairwise z-tests between each pair of k values.

For two measured means k_1 and k_2 with uncertainties σ_{k1} and σ_{k2}, the z-score is computed as:

$$z = \frac{|k_1 - k_2|}{\sqrt{\sigma_{k1}^2 + \sigma_{k2}^2}}$$

and if $z < 2$, the two measurements are statistically consistent at approximately a 95% confidence level.

Table 5: Pairwise z-tests between Week 1 and Week 2 spring constants k for all 5 configurations.

Configuration	$\lvert k_{W1} - k_{W2} \rvert$ (N/m)	Combined σ (N/m)	z
100 g, no plate	0.021	0.002	10.5
100 g, small plate	0.013	0.002	6.5
250 g, no plate	0.030	0.002	15.0
250 g, small plate	0.015	0.001	15.0
250 g, large plate	0.012	0.002	6.0

From the above data, we observe that all configurations differ by more than 2σ, though also need to keep in mind the fact that the magnitude of variation of the values of k (roughly between 5.16–5.50 N/m) is within about 7% of their mean. We can attribute the changing value of k as to the fact that we used the same spring for each of the 100 trials, and any observed variance likely arises from small changes in the equilibrium point as we continuously used it for heavier weights.

We next compare drag coefficients b between these 3 specific configurations:

Table 6: Targeted z-tests for drag coefficient b across specified configurations.

Configuration Pair	$\lvert b_1 - b_2 \rvert$ (kg/s)	Combined σ (kg/s)	z
100 g no plate – 250 g no plate	0.00131	0.00021	6.2
100 g small plate – 250 g small plate	0.00109	0.00031	3.5
250 g large plate – 250 g small plate	0.00931	0.00044	21.2

Similar to the spring constant data, we observe that all configurations differ by more than 2σ. To begin understanding this, it is important to first note that the damping coefficient b depends most notably on the cross-sectional area of the damping plate. For motion at relatively low speeds, according to NASA's beginners-guide-to-aeronautics, the drag force can be expressed as

$$F_d = bv = \frac{1}{2} C_d \rho A v^2,$$

where C_d is the drag coefficient and ρ is the air density. According to this, we expect the effective damping coefficient b to increase with the exposed surface area A since a larger plate interacts with a greater volume of air.

While the data trends generally support that b scales with area, variations across trials indicate that systematic effects also played a role. Examples of these are the fact that differences in how the plates are mounted and oriented on the weights could alter the effective cross-sectional area exposed to airflow. Any additional instability during oscillation where masses could rotate also can create a varying drag force, further increasing

our observed uncertainty.

For each of the five experimental configurations, we also analyzed the week 1 datasets using a non-linear chi-squared fit to the damped harmonic motion model:

$$x(t) = Ae^{-\alpha t}\sin(\omega t + \phi) + C, \tag{1}$$

The fit provides the values and uncertainties for each parameter, which we can use to compute the natural angular frequency ω_0, the spring constant k, and the drag coefficient b, as according to the same equations as used in the Introduction. The tables below summarize the results of z-tests between week 1 and week 2 data:

Table 7: Z-test for angular frequencies ω between week 1 and week 2.

Configuration	ω_{week1}	$\sigma_{\omega 1}$	ω_{week2}	$\sigma_{\omega 2}$	z	Agreement?
100 no plate	7.15662	0.00037	7.1566	0.00036	0.04	Yes
100 small plate	6.82330	0.00087	6.8273	0.00036	4.25	No
250 no plate	4.66016	0.00071	4.6512	0.00009	12.50	No
250 small plate	4.57107	0.00033	4.5708	0.00014	0.75	Yes
250 large plate	4.49380	0.00077	4.4986	0.00024	5.93	No

Table 8: Z-test for damping coefficients α between week 1 and week 2.

Configuration	α_{week1}	$\sigma_{\alpha 1}$	α_{week2}	$\sigma_{\alpha 2}$	z	Agreement?
100 no plate	0.006064	0.000380	0.006088	0.00036	0.05	Yes
100 small plate	0.042645	0.000907	0.041223	0.00036	1.46	Yes
250 no plate	0.005029	0.000394	0.0065184	0.000092	3.68	No
250 small plate	0.020530	0.000475	0.021696	0.00014	2.35	No
250 large plate	0.037032	0.000681	0.032157	0.00023	6.78	No

Table 9: Z-test for spring constants k between week 1 and week 2.

Configuration	k_{week1}	σ_{k1}	k_{week2}	σ_{k2}	z	Agreement?
100 no plate	5.24	0.00054	5.240	0.00038	0.00	Yes
100 small plate	5.16	0.0013	5.168	0.00054	5.70	No
250 no plate	5.50	0.0017	5.483	0.00021	9.99	No
250 small plate	5.37	0.00077	5.369	0.00033	1.19	Yes
250 large plate	5.42	0.0019	5.426	0.0014	2.54	No

Table 10: Z-test for drag coefficients b between week 1 and week 2.

Configuration	b_{week1}	σ_{b1}	b_{week2}	σ_{b2}	z	Agreement?
100 no plate	0.00124	0.00008	0.001247	0.000053	0.07	Yes
100 small plate	0.00946	0.00020	0.009143	0.000080	1.47	Yes
250 no plate	0.00255	0.00020	0.003303	0.000047	3.67	No
250 small plate	0.01055	0.00024	0.01114	0.000072	2.35	No
250 large plate	0.01986	0.00037	0.01725	0.00012	6.71	No

From these tables, we observe that several measured quantities between Week 1 and Week 2 agree within uncertainty, while others show statistically significant deviations. In general, configurations without plates tend to show more consistent angular frequencies and damping parameters across both weeks, while configurations with larger plates show larger discrepancies.

For the angular frequency ω, two out of five configurations agree between Week 1 and Week 2, while the remaining three show z-scores greater than 2, indicating statistically significant differences. The largest discrepancies occur for the 250 g no plate and 250 g large plate configurations, which may result from the varies initial displacement we had set. The same trend holds for the spring constant k, since it is a direct derivation from ω.

For the damping constant α, the 100 g no plate and 100 g small plate configurations show good agreement, while the three 250 g configurations disagree. This pattern suggests that unlike with lighter systems, the heavier systems (especially with plates attached) experience more complex air drag behavior that deviates from ideal linear damping. The same reasons are also present in what affects the drag coefficient b, as specific variability in air resistance and turbulent effects are difficult to precisely reproduce across separate weeks.

Now given these observations, we can reassess the agreement level between our spring constant and drag coefficient measurements across both weeks by using Week 1 values of k and incorporating the Week 2 standard deviations as uncertainties as according to the following equation:

$$z = \frac{|k_1 - k_2|}{\sqrt{\sigma_1^2 + \sigma_2^2}}.$$

Recomputing the pairwise comparisons across all configurations yields us with the following table:

Table 11: Spring constant comparisons using Week 1 fit values with Week 2 standard deviations.

Comparison	$k_1 - k_2$ (N/m)	σ_{combined} (N/m)	Significance (σ)
250g Large vs 250g Small	0.057	0.00205	27.8
250g Large vs 250g No Plate	-0.057	0.00255	22.4
250g Large vs 100g Small	0.258	0.00230	112.2
250g Large vs 100g No Plate	0.186	0.00197	94.4
250g Small vs 250g No Plate	-0.114	0.00186	61.3
250g Small vs 100g Small	0.201	0.00151	133.1
250g Small vs 100g No Plate	0.129	0.00094	137.2
250g No Plate vs 100g Small	0.315	0.00214	147.2
250g No Plate vs 100g No Plate	0.243	0.00178	136.5
100g Small vs 100g No Plate	-0.072	0.00141	51.1

Even with the updated Week 2 uncertainties, all the spring constant comparisons remain statistically inconsistent with each other with z-scores ranging from 22σ to 147σ. The trend of higher effective spring constants for the 250g configurations persists, further suggesting systematic factors as already discussed being prevalent.

We can do the same for drag coefficient values and display our results below:

Table 12: Drag coefficient comparisons using Week 1 single-fit values with Week 2 standard deviations.

Comparison	$\lvert b_1 - b_2 \rvert$ (kg/s)	σ_{combined} (kg/s)	Significance (σ)
No damper: 100g vs 250g	0.002056	0.000216	9.5
Small damper: 100g vs 250g	0.001997	0.000312	6.4
250g: Small vs Large Plate	0.00611	0.000442	13.8

The drag coefficient comparisons also show large statistical differences, confirming that plate area still indeed has a measurable impact on the damping behavior of the oscillator. Although we notice that relative to our original analysis our significance levels are modestly reduced, this still doesn't affect the fact that both analyses reveal disagreements stem primarily from systematic effects such as air resistance modeling and geometric variations, thus strengthening our claim that the major sources of deviation are systematic instead of random.

To further analyze the variability in our measurements, histograms of the fitted damping constant α and the damped frequency ω are plotted for each configuration as shown below.

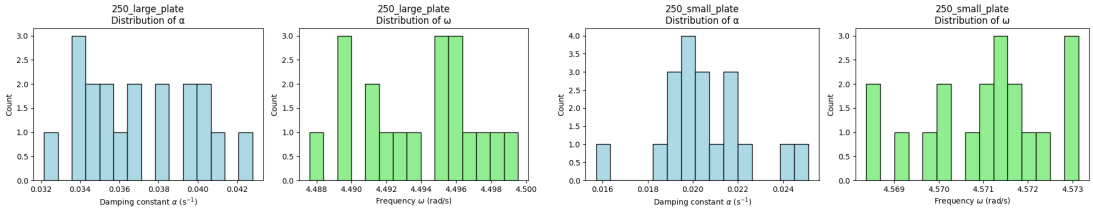

Figure 1: Distributions of α and ω with Left: 250g Large Plate; Right: 250g Small Plate.

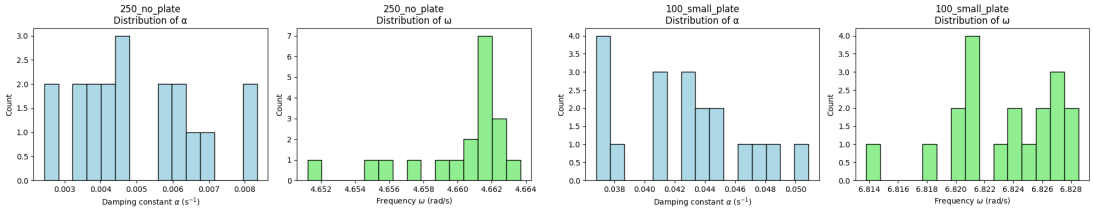

Figure 2: Distributions of α and ω with Left: 250g No Plate; Right: 100g Small Plate.

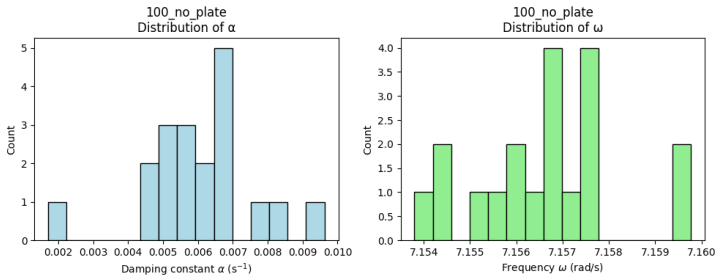

Figure 3: Distributions of α and ω with 100g No Plate.

As seen in the plots, the distributions for α and ω generally appear approximately Gaussian, with some slight skewness or flattening in certain configurations. This variation is expected given the limited number of trials per setup, as we had only 20 independent runs for each configuration. According to the Central Limit Theorem, the sampling distribution of the mean approaches normality as the number of samples increases, typically requiring at least 30 independent trials for the approximation to hold reliably. Therefore, our small deviations from ideal Gaussian shapes here are consistent with statistical expectations for $N = 20$. Overall however, the spread of each histogram being approximately gaussian confirms our expectations that our z-tests indeed can be used as valid sources of statistical analysis as we have done above.

3 Discussion and Conclusion

The primary outcome of this experiment is that we successfully showed that the simple damped harmonic oscillator models the behavior of our mass-spring system across all configurations well. The extracted spring constants k and drag coefficients b reveal significant systematic deviations that exceed the statistical uncertainties from the fits. Specifically, all five spring constant configurations differ by z-scores ranging from 22σ to 147σ, with 250 g configurations consistently exhibiting higher k values (5.37–5.50 N/m) compared to 100 g configurations (5.16–5.24 N/m). This indicates that systematic effects related to mass, such as more complex air drag behavior and nonideal spring behavior under larger masses, influence the measured values.

For the damping coefficient b, larger plates increased damping as expected, but configurations with identical plates still displayed discrepancies between 100 g and 250 g masses (3.5σ–6.4σ). These differences likely arise from variations in plate mounting and orientation, oscillation instability, or slight rotations of the mass during motion, all of which change the effective cross-sectional area exposed to airflow by creating more complicated drag flow.

Comparing our Week 1 single-fit results to our 20-trial Week 2 fits reveals agreements such as the fact that our 100 g no plate configurations match well across all parameters, while other configurations (with especially the 250 g large plate) show significant differences, demonstrating just how much systematic effects can dominate.

Histograms of α and ω for each configuration were approximately Gaussian, with minor skewness or flattening consistent with having only 20 trials per setup. These deviations made sense as according to the Central Limit Theorem's [3] requirement of at least 30 independent trials to approach normality. Therefore, the observed deviations from ideal Gaussian shapes are expected, and our approximate Gaussian spread confirms that z-tests provide a valid statistical framework for assessing agreement across configurations.

Further thought in the sources of our observed discrepancies reveal that it can be attributed to several factors, such as the fact that the spring's mass must be accounted for as well in our calculations and that our real world spring doesn't exhibit ideal behavior, which may have caused k to appear dependent on the mass and produce lower values for lower masses. Additionally, small misalignments in spring or plate mounting, and the tendency of lighter masses to oscillate or rotate more easily due to their decreased inertia can introduce further systematic noise. Lastly, variations in initial plate orientation and mass geometry directly alter the effective cross-sectional area exposed to airflow, resulting

in differing drag forces even for identical configurations.

Overall, while our experiment confirmed the qualitative behavior of damped harmonic motion, the dominant source of uncertainty arose from these systematic effects, highlighting the importance of considering real-world deviations from ideal models that we see in theory.

References

[1] I. Hughes and T. Hase, *Measurements and their Uncertainties: A Practical Guide to Modern Error Analysis*, Oxford University Press, 2010.

[2] NASA Glenn Research Center, "Drag Equation," *Beginner's Guide to Aerodynamics*, NASA, `https://www.grc.nasa.gov/www/k-12/airplane/drageq.html`.

[3] S. G. Kwak and J. H. Kim, "Central limit theorem: the cornerstone of modern statistics," *Korean Journal of Anesthesiology*, vol. 70, no. 2, pp. 144–156, 2017. [Online]. Available: `https://www.ncbi.nlm.nih.gov/pmc/articles/PMC5370305/`